DOI 10.5012/bkcs.2010.31.5.1331

Preparation and Characterization of Spherical Carbon Composite for Use as Anode Material for Lithium Ion Batteries

Byoung-hoon Ahn and Sung-Man Lee*

*Department of Advanced Materials Science and Engineering, Kangwon National University, Chuncheon, Kangwon-Do 200-701, South Korea. *E-mail: smlee@kangwon.ac.kr*
Received January 28, 2010, Accepted March 18, 2010

A novel spherical carbon composite material, in which nanosized disordered carbons are dispersed in a soft carbon matrix, has been prepared and investigated for use as a potential anode material for lithium ion batteries. Disordered carbons were synthesized by ball milling natural graphite in air. The composite was prepared by mixing the ball-milled graphite with petroleum pitch powder, pelletizing the mixture, and pyrolyzing the pellets at 1200 °C in an argon flow. The ball-milled graphite consists of distorted nanocrystallites and amorphous phases. In the composite particle, nanosized flakes are uniformly distributed in a soft carbon matrix, as revealed by X-ray diffractometer (XRD) and transmission electron microscopy (TEM) experiments. The composite is compatible with a pure propylene carbonate (PC) electrolyte and shows high rate capability and excellent cycling performance. The electrochemical properties are comparable to those of hard carbon.

Key Words: Lithium-ion battery, Anode material, Carbon composite, Electrochemical performance

Introduction

Lithium-ion batteries are widely used in various portable electronic devices. Recently, there has been extensive research and development work on future applications of these batteries, such as in hybrid electric vehicles and electric vehicles. These high-power applications depend on the high rate capability of the batteries. Highly crystalline graphite is currently used as the anode (the negative electrode) in lithium ion batteries due to its very flat potential and structural stability upon cycling. However, since the rate capability is lower in more highly crystalline carbons, disordered carbons such as hard carbon and soft carbons pyrolyzed at low temperatures have attracted much attention as a promising anode material for Li-ion batteries to be used in high-power applications.[1,2] In addition, these disordered carbons are stable during charge-discharge cycling in PC-based electrolytes (which are attractive due to their low melting points), whereas graphites are incompatible with PC-based electrolytes due to rapid electrolyte decomposition and exfoliation of the graphite structure.[3,4]

It is known that spherically shaped material is preferable as a means of improving anode characteristics due to its high tapping density.[5] Unfortunately, the morphology of disordered carbons is usually irregular.

In general, diffusion in a solid (i.e., the mass transport of lithium ions within the carbon) is a slow process. Thus the diffusion rate would dominate the overall reaction rate for Li insertion and extraction. Nanosized materials are the most promising materials for high-power applications because of the short path length for lithium ion diffusion.[6,7] In view of these considerations, a disordered carbonaceous material with fine particles would appear to be attractive for high-power applications. Nevertheless, anode materials with a small particle size show a large, irreversible capacity loss during initial cycling. This loss is mainly caused by electrolyte decomposition and the formation of a passivation film on the particles, and limits the applicability of fine anode materials. This irreversible capacity loss can be reduced by pelletizing the fine carbon particles with a soft carbon.

On the other hand, mechanical milling of graphite is one possibility of producing disordered carbons,[8-13] in which the milling of graphite powder under drastic conditions or for long durations leads to highly disordered carbons with a particle size of few nanometers and nanosized crystallites.

With these considerations in mind, we have sought to prepare fine disordered-carbon particles using a mechanical milling process, and to subsequently pelletize them with soft carbons such as pitch-based carbons to obtain a spherical carbon composite.

In this work, we prepared a novel spherical composite anode material consisting of nanosized disordered carbon particles in a soft carbon matrix. We then investigated the structural and morphological characteristics and the electrochemical performance of this composite.

Experimental Procedures

The disordered carbon samples of the present work were prepared by ball milling high purity (99%) natural graphite under an air atmosphere. The ball milling was carried out in a planetary ball-mill (pulverisette-7, Fritsch) with hardened steel vial and balls (diameter: 5 mm, 10 mm). The ratio of the ball mass to graphite powder was 20:1. A spherical carbon composite was prepared as follows. The ball-milled graphite powders were mixed with petroleum pitch powders (70:30 by weight) in a planetary ball mill. The mixture was pelletized into spherical-shaped composite powders in an homemade agglomerator, followed by heating at 1200 °C for 1 h under an argon atmosphere.

The structural changes of the ball-milled and composite powders were characterized using an XRD with Cu Kα radiation. The particle size distribution was analyzed by a laser particle size analyzer (Mastersizer 2000, Malvern). The cross-sec-

tional image and microstructure of the composite particle were examined by scanning electron microscopy (SEM) and TEM, respectively. The sample for TEM analysis was prepared using a focused ion beam (FIB) workstation. For electrochemical measurements, half-cells using a 2016-type coin cell were assembled in an Ar-filled glove box with a lithium foil counter electrode and a working electrode. The working electrode was prepared by pasting a slurry of 95 wt % active material and 2.5 wt % styrene butadiene rubber (SBR) as a binder, dissolved in 2.5 wt % carboxy methyl cellulose (CMC) water solution, onto a copper foil, followed by drying in vacuum at 180 °C for 12 h.

The electrolytes were 1 M $LiPF_6$ in a mixture of ethylene carbonate (EC) and diethyl carbonate (DEC) (1:1 by volume) and 1 M $LiClO_4$ dissolved in propylene carbonate (PC) (provided by Ukseung Chemical Co., Ltd., Korea). The cells were charged (intercalated) and discharged (deintercalated) between 0.005 V and 2.0 V at 30 °C. In order to determine the capacity and cycle performance, the cells were charged in a constant current-constant voltage (CC-CV) mode consisting of a constant current at 0.2 mA/cm^2 followed by a constant voltage at 0.005 V until the current tapered down to 0.01 mA. The cells were discharged at a constant current of 0.2 mA/cm^2. To measure the rate capability, the cells were charged in the CC-CV mode and discharged in the CC mode at different rates between 0.2 C and 10 C.

Results and Discussion

Fig.1 shows typical SEM images of the as-received natural graphite, a sample milled in an air atmosphere for 2 h, and a carbon composite prepared by pelletizing a mixture of ball-milled graphite and petroleum pitch powders and heating the pellets at 1200 °C for 1 h in an argon atmosphere. Typical image of hard carbon is given for comparison. The as-received graphite particles have an average size of approximately 6 μm, as shown in Fig. 1(a). The ball-milled natural graphite powders are composed of sub-micron agglomerates (Fig.1(b)). Fig.1(c) shows the spherical morphology of the composite powders, while hard carbon has irregular shapes with sharp edges. The particle size distributions of the as-received natural graphite, the ball-milled graphite, and the composite powder are shown in Fig. 2. The average particle size of as-received natural graphite is 6 μm. For ball-milled samples, the size distribution is bimodal with peaks at 0.15 μm and 1.2 μm. On the other hand, the average particle size of the composite powder is 7.9 μm.

XRD patterns of the as-received natural graphite, the ball-milled graphite and the composite are given in Fig. 3. The as-received natural graphite is very well-crystallized. After ball-milling, Bragg peaks are significantly broadened and weakened. This indicates that the graphite is disordered as a result of ball milling, as previously reported.[8-13] The broadened peak corresponding to the (002) reflection peak is asymmetric and may be divided into two components, one of which might correspond to an interlayer spacing, d_{002}, of 0.353 nm of relatively ordered graphite crystals, and another which relates to a larger interlayer spacing of lattice-damaged crystals.[14] As shown in Fig. 4, this is confirmed by a high-resolution electron microscopy (HREM) image of the ball-milled sample, consisting of crumpled lamellae with a nanocrystal size (see area A) and amorphous carbon (see area B). It has been known that graphite, during high-energy ball milling, undergoes a crystal-nanocrystal-amorphous transition.[15] The XRD pattern of the carbon composite in Fig. 3(c) shows that the (002) diffraction peak of graphite has not been recovered after annealing at 1200 °C. Note that iron impurities from the steel vial and balls during milling results in the formation of crystalline iron carbide (Fe_3C) upon subsequent heat treatment.

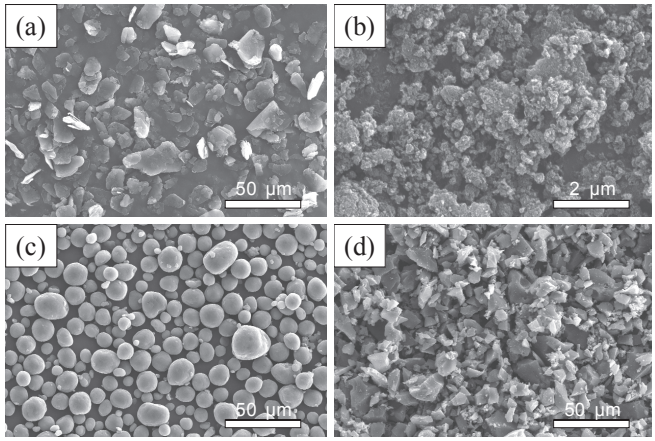

Figure 1. SEM micrographs of (a) as-received natural graphite, (b) ball-milled graphite, (c) nanocrystalline graphite/carbon composite and (d) hard carbon.

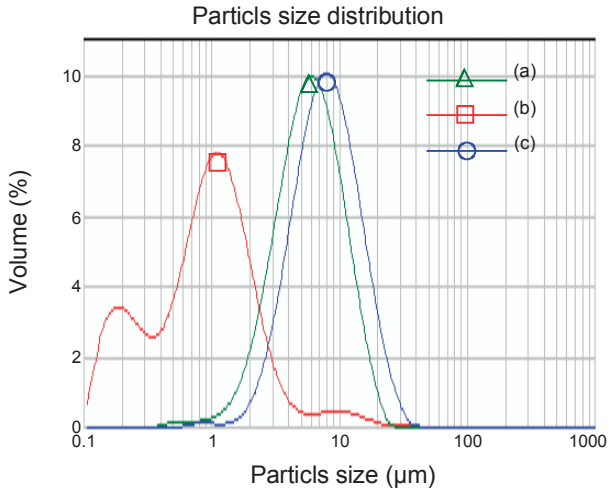

Figure 2. Particle size distributions of (a) as-received natural graphite, (b) ball-milled graphite, and (c) graphite/carbon composite.

The electron diffraction pattern for an image of the composite depicted in Fig. 5 is also characterized by diffuse rings (see inset of Fig. 5). This means that a transformation from an amorphous (or distorted nanocrystallites) to a layered graphite structure does not occur significantly after heat treatment at 1200 °C. In the TEM image of the composite (Fig. 5), nanosized flakes are uniformly distributed in a soft carbon matrix.

Fig. 6 shows the cross-sectional image of a composite sphere, which was obtained using a FIB workstation. It appears that the composite sphere has a quite dense internal structure though some nanosized holes are observed inside the sphere.

Fig. 7 shows the electrochemical charge and discharge curves

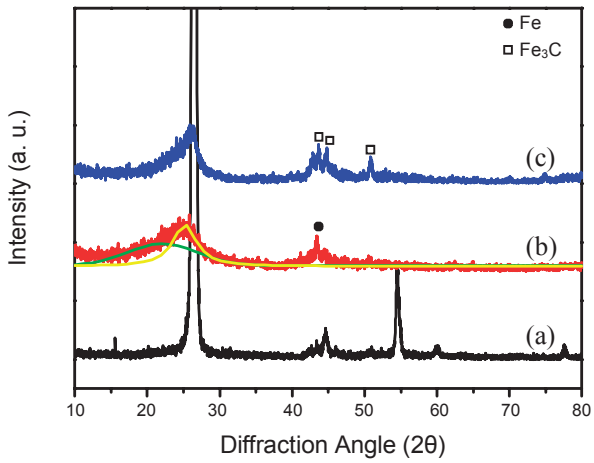

Figure 3. XRD patterns of (a) as-received natural graphite, (b) ball-milled graphite, and (c) graphite/carbon composite.

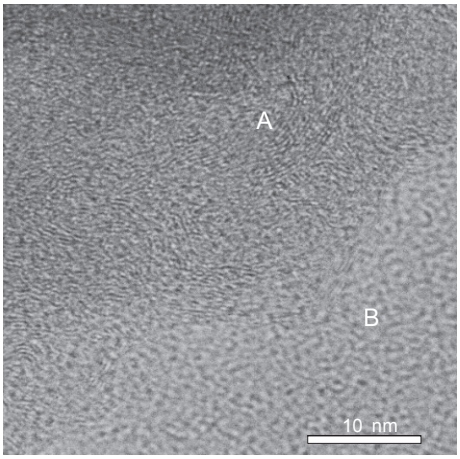

Figure 4. High-resolution electron microscopy (HREM) images of ball-milled graphite. (A: crumpled lamellae with nanocrystal size and B: amorphous carbon)

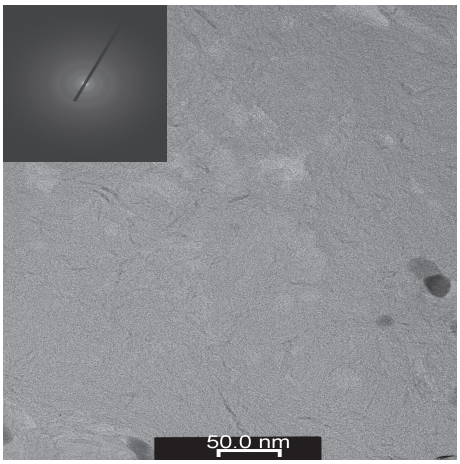

Figure 5. HREM image of nanocrystalline graphite/carbon composite sphere and its selected area diffraction pattern (inset).

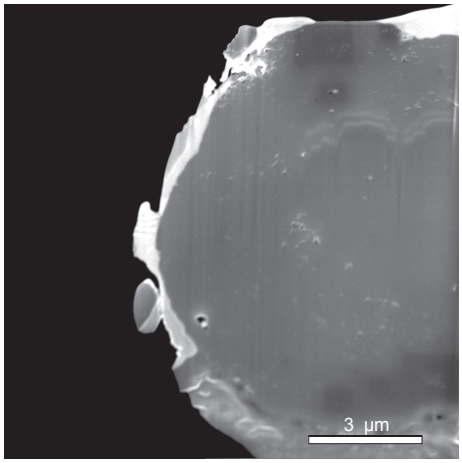

Figure 6. Cross-sectional image of nanocrystalline graphite/carbon composite sphere.

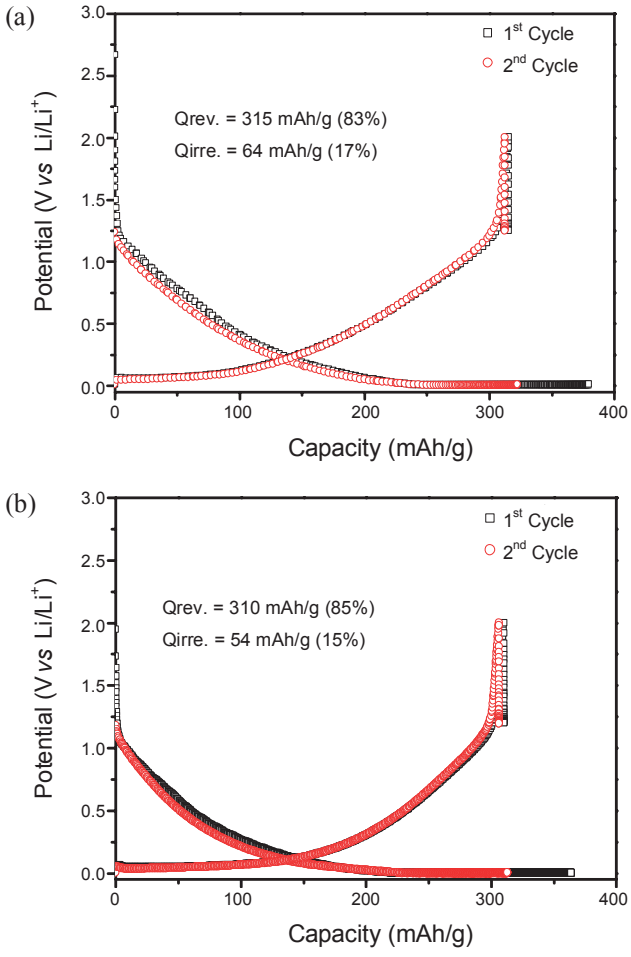

Figure 7. Charge-discharge curves for the first two cycles : (a) hard carbon and (b) carbon composite.

of commercial hard carbon (average particle size: 7.8 μm, Kureha Corp., Japan) and the carbon composite for the first two cycles. Apparently, the charge-discharge profiles of the composite electrode are similar to that observed in typical hard carbon

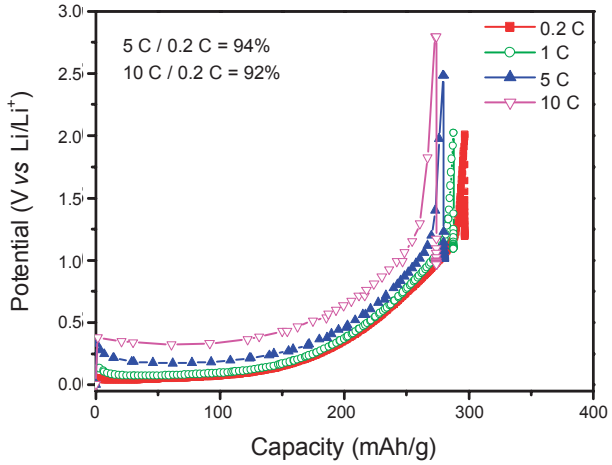

Figure 8. Discharge curves of carbon composite for selected current rates.

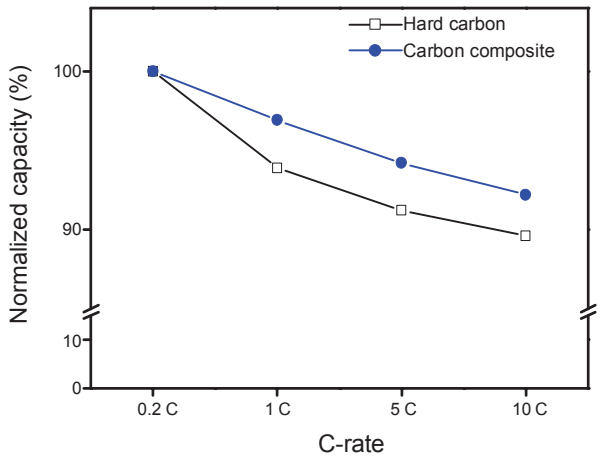

Figure 9. Comparison of rate capabilities of carbon composite and commercial hard carbon.

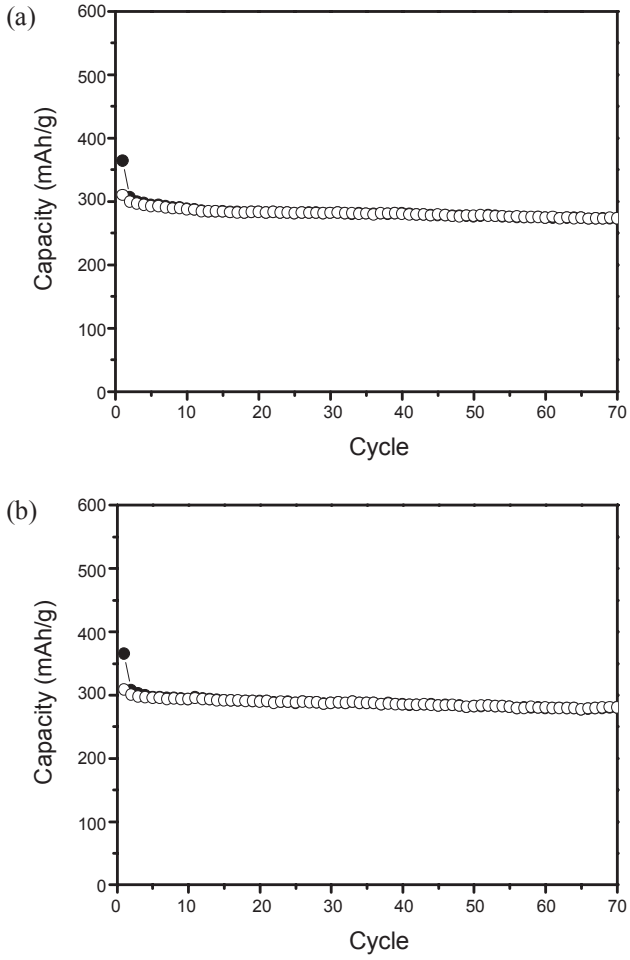

Figure 10. Cycling performance of composite sample for two different electrolytes: (a) 1 M $LiPF_6$ EC/DEC and (b) 1 M $LiClO_4$ PC.

possessing the disordered structure. The initial coulombic efficiency is 83 and 85% for hard carbon and carbon composite, respectively. Fig. 8 shows the discharge curves for selected current rates (up to 10 C) of the composite electrode. The overpotential of the composite electrode is low at discharge rate up to 5 C. In Fig. 9, a comparison of the rate capability data for the carbon composite and commercial hard carbon is shown. The electrode loading was 3.8 mg/cm^2 and 3.7 mg/cm^2 for the composite and hard carbon electrodes, respectively. It appears from Fig. 9 that the discharge rate capability of the carbon composite electrode is better than that for the hard carbon electrode.

Fig. 10 shows the cycling performance of the composite sample for the two different electrolytes of 1 M $LiPF_6$ EC/DEC and 1 M $LiClO_4$ PC. The composite electrode maintains quite stable capacity during cycling even in an electrolyte with a pure PC solvent. It is noteworthy that the electrochemical performance characteristics of the composite electrode, such as its charge/discharge potential profile and initial coulombic efficiency, are almost identical for the two electrolytes. These preliminary results suggest that the carbon composite is a promising alternative to hard carbons as an anode material in lithium ion batteries for high-power applications.

Conclusion

Spherical carbon composites, as potential anode materials for lithium ion batteries, were prepared by mixing ball-milled graphite and petroleum pitch powders in a planetary ball-mill, followed by pelletizing and heat treatment at 1200 °C for 1 h in an argon flow. The ball-milled graphite consists of distorted nanocrystallites and amorphous phases. In composite particles, nanosized flakes are uniformly distributed in the soft carbon matrix, as revealed by the XRD and TEM experiments. It was found that the composites were compatible with a pure PC electrolyte and exhibited high rate capability and good cyclability.

Acknowledgments. This work was supported by the Korea Research Foundation Grant from the Korean Government (MEST) (The Regional Research Universities Program/Medical & Bio-Materials Research Center) and the Division of Advanced Batteries under the NGE Program (Project No: 10016446).

References

1. Zaghib, K.; Brochu, F.; Guerfi, A.; Kinoshita, K. *J. Power Sources* **2001**, *103*, 103.
2. Horiba, T.; Maeshima, T.; Matsumura, T.; Koseki, M.; Arai, J.; Muranaka, Y. *J. Power Sources* **2005**, *146*, 107.
3. Arakawa, M.; Yamaki, J. *J. Electroanal. Chem.* **1987**, *219*, 273.
4. Chung, G.; Jun, S.; Lee, K.; Kim, M. *J. Electrochem. Soc.* **1999**, *146*, 1664.
5. Yoshio, M.; Wang, H.; Lee, Y. S.; Fukuda, K. *Electrochim. Acta* **2003**, *48*, 791.
6. Habazaki, H.; Kiriu, M.; Konno, H. *Electrochem. Commun.* **2006**, *8*, 1275.
7. Bueno, P. R.; Leite, E. R. *J. Phys. Chem. B* **2003**, *107*, 8868.
8. Fukunaga, T.; Nagano, K.; Mizutani, U.; Wakayama, H.; Fukushima, Y. *J. Non-Cryst. Solids* **1998**, *232-234*, 416.
9. Wakayama, H.; Mizuno, J.; Fukushima, Y.; Nagano, K.; Fukunaga, T.; Mizutani, U. *Carbon* **1999**, *37*, 947.
10. Ong, T. S.; Yang, H. *Carbon* **2000**, *38*, 2077.
11. Lee, K. M.; Oh, S. M.; Lee, S. M. *Bull. Korean Chem. Soc.* **2008**, *29*, 1121.
12. Welham, N. J.; Berbenni, V.; Chapman, P. G. *J. Alloy Compd.* **2003**, *349*, 255.
13. Natarajan, C.; Fujimoto, H.; Mabuchi, A.; Tokumitsu, K.; Kasuh, T. *J. Power Sources* **2001**, *92*, 187.
14. Aladeromo, J. B.; Bragg, R. H. *Carbon* **1990**, *28*, 897.
15. Zhou, W. L.; Ikuhara, Y.; Zhao, W.; Tang, J. *Carbon* **1995**, *33*, 1177.